

Supplementary data file

Spin-lattice correlations in Eu³⁺-doped antiferromagnet TmFeO₃

Poorva Sharma,^{a, b} Arvind Yogi,^c Ashwini Kumar,^{d, e} Rubin Li,^a Gaurav Sharma,^f

Jiyu Fan,^b Vasant Sathe,^f Qi Li,^d Wei Ren,^{*a} and Shixun Cao ^{†a}

^aDepartment of Physics, International Center for Quantum and Molecular Systems, Shanghai University,
Shangda Road 99, Shanghai 200444, China

^bDepartment of Applied Physics, Nanjing University of Aeronautics and Astronautics, Nanjing 210016, China

^cMax-Planck-Institut für Festkörperforschung, Heisenbergstr. 1, D-70569 Stuttgart, Germany.

^dSchool of Physics, Southeast University, Jiangning District, Nanjing, 211189, China

^eSchool of Chemistry and Chemical Engineering, Southeast University, Jiangning District, Nanjing, 211189, China

^fUGC-DAE Consortium for Scientific Research, Devi Ahilya University Campus, Khandwa Road, Indore, 452001, India

(Dated: July 22, 2019)

*renwei@shu.edu.cn, †sxcao@shu.edu.cn

Supplementary Information (SI-1)

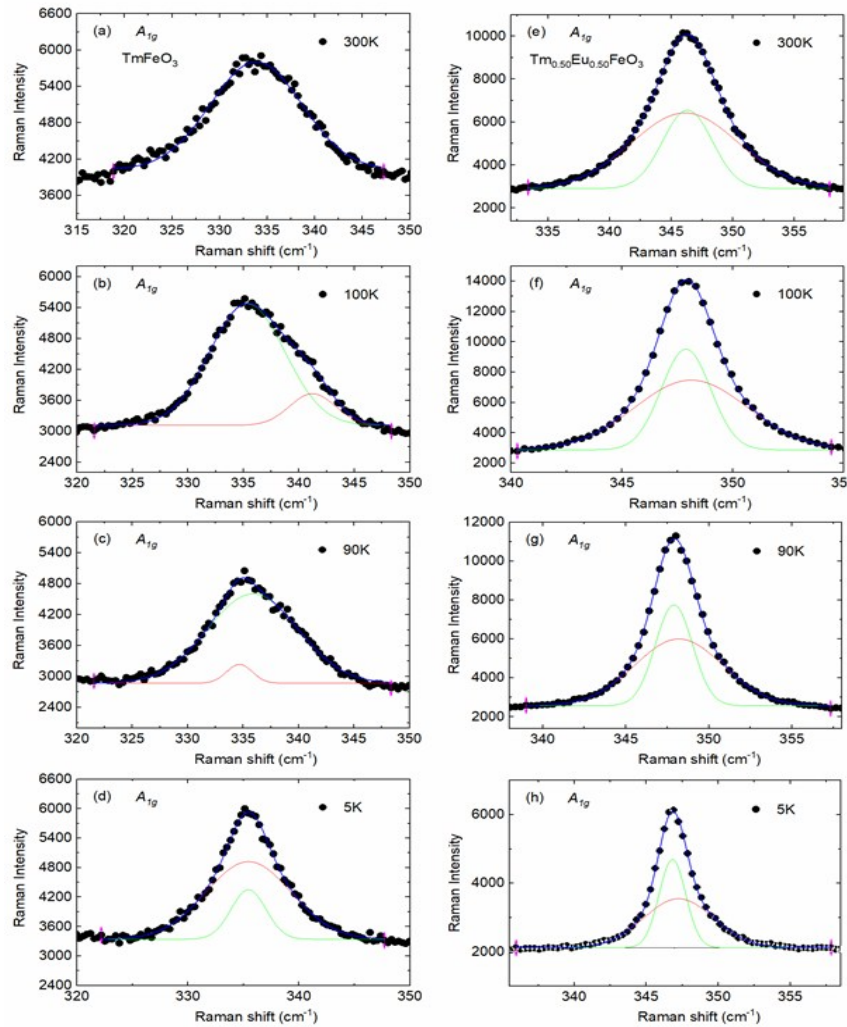


Fig. S1: Representation of Raman-active phonon modes for TmFeO_3 (a, b, c, d) and $\text{Tm}_{0.5}\text{Eu}_{0.5}\text{FeO}_3$ (e, f, g, h) compounds at different temperatures of 5, 90, 100 and 300K. The Raman spectra was acquired at excitation wavelength $\lambda_{\text{exc}} = 633 \text{ nm}$.

The lattice phonon modes are strongly coupled with magnetic ordering and show a clear sharp change near the transition as indicated by the light yellow vertical box as represented in manuscript in Fig. 5. Despite the clear change in Raman shift as a function of temperature are evident near the spin-reorientation transition, Raman scattering process are significantly different for the both compounds near the Raman-active phonon modes as a function of temperature as shown in Supplementary Information (SI-1), Fig. S1, Table S1 and S2. This indicates substitution of Eu³⁺ at Tm³⁺ ion in TmFeO₃ strongly influenced magnetic properties through magnon-phonon (spin-lattice) coupling.

Table S1: Raman-active phonon modes as a function of temperature for TmFeO₃ compound.

Temperature (K)	A _{1g} /B _{1g}	A _{1g}	B _{1g}	B _{1g}	A _{1g}	B _{2g}	A _{1g} /B _{2g} /B _{3g}	B _{2g}	A _{1g} /B _{1g}	B _{1g}	Two phonon
	(cm ⁻¹)										
5	113.042	--	161.861	--	335.122	359.3	430.747	--	469.361	491.235	--
10	113.042	--	161.861	--	335.122	359.3	430.747	--	469.043	491.235	--
15	113.042	--	161.861	--	335.122	359.256	430.747	--	469.043	491.235	--
20	112.366	--	161.861	--	335.122	359.256	430.747	--	469.043	491.235	--
25	112.704	--	161.861	--	335.122	359.256	430.747	--	469.043	491.551	--
30	113.042	141.048	161.861	--	335.122	359.256	430.747	--	469.043	491.551	--
35	113.042	141.048	161.861	--	335.122	359.256	430.747	--	469.043	491.551	--
40	113.042	141.048	161.861	--	335.122	359.256	430.747	--	469.043	490.919	--
45	113.042	141.048	161.861	--	335.122	357.651	430.747	--	469.043	490.919	--
50	113.042	141.048	161.861	--	335.122	357.651	430.747	--	469.043	490.919	--
55	113.042	141.048	161.861	--	335.122	357.651	430.747	--	469.043	490.919	--
60	113.042	141.048	161.861	--	335.122	357.651	430.747	--	469.043	490.919	--
65	113.042	141.048	161.861	--	335.122	357.651	430.747	--	469.043	490.919	--
70	113.042	141.048	161.861	--	335.122	357.651	430.747	--	469.043	490.919	--
80	113.042	141.048	161.861	--	334.479	357.651	430.747	--	469.043	490.919	--
90	113.042	141.048	161.861	--	335.445	358.293	430.747	--	469.043	490.919	--
100	113.042	141.048	161.861	--	335.445	358.293	430.747	--	469.043	490.919	--
110	113.042	141.048	161.861	--	335.445	357.972	429.464	--	469.043	490.919	--
150	112.862	141.209	161.5903	--	336.413	357.972	427.633	--	469.78	490.919	--
200	112.862	141.209	161.1702	--	335.638	357.847	426.35	--	469.78	491.657	--
250	111.846	141.209	160.684	--	333.702	356.563	424.681	--	467.237	489.758	--
300	111.846	141.209	160.35	--	333.702	356.563	424.103	--	467.237	489.758	--
											625.788
											1289.11

Table S2: Raman-active phonon modes as a function of temperature for $Tm_{0.5}Eu_{0.5}FeO_3$ compound.

Temperature	A_{1g}/B_{1g}	A_{1g}	B_{1g}	B_{1g}	A_{1g}	B_{2g}	$A_{1g}/B_{2g}/B_{3g}$	B_{2g}	A_{1g}/B_{1g}	B_{1g}	Two phonon
(K)	(cm ⁻¹)										
5	111.854	145.587	163.36	325.618	347.876	367.788	436.192	483.755	510.179	632.366	--
10	112.192	145.587	163.36	325.434	347.876	367.788	436.192	483.755	510.179	632.366	--
15	112.366	145.083	163.36	325.434	347.876	367.788	436.192	482.331	510.129	631.578	1277.4
20	112.366	145.083	163.36	325.434	347.876	367.788	436.192	482.331	510.76	631.578	1277.4
25	112.028	145.083	163.36	325.434	347.876	367.788	436.192	482.371	511.113	631.612	1277.4
30	112.028	145.083	163.36	325.434	347.876	367.788	436.192	482.371	511.113	631.612	1277.4
35	112.028	145.083	163.36	325.434	347.876	367.788	436.192	482.371	511.113	631.612	1277.4
40	112.028	145.083	163.36	325.434	347.876	367.788	436.192	482.371	511.113	631.612	1277.4
45	112.028	143.402	163.36	325.434	347.876	367.788	436.192	482.371	511.113	631.612	1277.4
50	112.028	143.402	163.36	324.463	347.876	367.788	436.192	482.371	511.113	631.612	1277.4
55	112.028	143.402	163.36	324.463	347.876	367.788	436.192	482.371	511.113	631.612	1277.4
60	112.028	141.384	163.36	324.463	347.876	367.788	436.192	482.371	511.113	631.612	1277.4
65	112.028	141.384	163.36	324.463	347.876	367.788	436.192	482.371	511.113	631.612	1277.4
70	112.028	141.384	163.36	324.463	347.876	367.788	436.192	482.371	511.113	631.612	1277.4
80	112.028	140.375	163.36	324.463	347.876	367.788	436.192	482.371	511.113	631.612	1277.4
90	112.028	140.375	163.36	324.463	347.876	367.788	436.192	482.371	511.113	631.612	1277.4
100	112.366	140.271	163.36	324.463	347.876	367.788	436.192	482.371	511.113	631.612	1295.76
110	112.366	139.365	161.405	323.817	347.891	367.788	436.192	482.371	511.113	631.693	1297.12
150	112.524	138.853	162.043	323.817	347.695	367.788	437.246	483.427	511.854	631.752	1297.32
200	111.846	138.18	162.456	324.331	347.191	367.788	437.246	483.427	510.595	631.752	1297.32
250	111.508	137.843	162.827	324.331	346.581	367.788	437.246	483.427	508.074	631.752	1297.32
300	111.508	137.843	163.222	324.331	345.951	367.788	437.246	483.427	508.074	631.752	1297.32

Supplementary Information (SI-2)

We have calculated bond-length, bond-angle as shown in Table S3 by using Fullprof software [1]. Further, the change in the rotation and distortion associated with FeO_6 octahedra also leads to the change in the Fe–O–Fe bond-angles, Fe–O bond-lengths and Fe–Fe atom distance. Again, in perovskite systems it is important to note that the tilt angles (rotation with FeO_6), Fe–O bond-length and Fe–O–Fe angle can be tuned either by external pressure or by doping of ions at crystallographic R/Fe-sites. Therefore, Eu doping at Tm-sites can change these parameters strongly and can affects the physical properties. Here, we have also calculated the tilting angles by using the related unit-cell metrics [2].

Table S3: Bond-lengths (\AA), bond, and tilt-angles (degree).

Tm FeO_3	Tm $_{0.50}\text{Eu}_{0.50}\text{FeO}_3$
Tm-O1 = 2.627	Tm-O1 = 2.6608
Tm-O1 = 2.329	Tm-O1 = 1.703
Tm-O2 = 2.2903	Tm-O2 = 2.759
Tm-O2 = 2.145	Tm-O2 = 2.35
	Tm-O2 = 2.146
Fe-O1 = 2.0199	Tm-O2 = 2.709
Fe-O1 = 1.9626	
Fe-O2 = 2.0373	Fe-O1 = 2.2473
	Fe-O2 = 1.80760
Fe-O1-Fe = 148.38°	Fe-O2 = 2.0747
Fe-O2-Fe = 137.47°	
	Fe-O1-Fe = 116.57°
	Eu-O1-Eu = 136.41°
	Eu-O2-Eu = 169.72°
	Fe-O2-Fe = 169.172°
Tilt-angles for Tm FeO_3	Tilt-angles for Tm $_{0.50}\text{Eu}_{0.50}\text{FeO}_3$
$\theta_{\text{oct}} = (180 - 148.38)/2 = 31.72$	$\theta_{\text{oct}} = (180 - 116.57)/2 = 31.72$
$\phi_{\text{oct}} = (180 - 137.47)/2 = 21.265$	$\phi_{\text{oct}} = (180 - 169.72)/2 = 5.14$
$\theta_{\text{oct}} = \cos^{-1}(a/b) = \cos^{-1}(0.94209) = 19.59$	$\theta_{\text{oct}} = \cos^{-1}(a/b) = \cos^{-1}(0.94209) = 18.214$
$\phi_{\text{oct}} = \cos^{-1}(\sqrt{2}a/c) = \cos^{-1}(0.9786) = 11.8746$	$\phi_{\text{oct}} = \cos^{-1}(\sqrt{2}a/c) = \cos^{-1}(0.9786) = 10.275$

Reference:

- [1] J. Rodriguez-Carvajal, Recent advances in magnetic structure determination by neutron powder diffraction, *Physica B: Condensed Matter* 192, 55 (1993).
- [2] Yusheng Zhao, Donald J. Weidner, John B. Parise, and David E. Cox, *Phys. of the Earth and Planetary Interiors*, 76, 1—16 (1993).